

# Precision design aspects for friction actuation with error compensation<sup>†</sup>

Samir Mekid\*

Department of Mechanical Engineering, King Fahd University of Petroleum & Minerals, Dhahran, 31260, KSA

(Manuscript Received February 4, 2008; Revised December 16, 2008; Accepted June 8, 2009)

---

## Abstract

Some key aspects in the design of actuators for ultra precision systems will require particular attention as actuators have to comply with ultra precision positioning and related tight specifications. The actuation is an important sub-group within the overall system to be designed. Any design failure in this sub-group will degrade drastically the machine performance. An interface analysis with immediate surrounding sub-groups is important to secure better generation of motion. In this paper, a design procedure for an actuator dedicated to generate high precision motion is presented with a discussion of some important aspects encountered when designing a friction drive. The procedure encompasses design concepts, axis stiffness, control, system dynamics, and, error compensation using a dedicated control strategy compensating for errors. A case study is discussed.

**Keywords:** Actuators; Friction drive; Design; Precision positioning

---

## 1. Introduction

Achieving ultra precision motion is not an easy task for engineers when designing precision machines. A machine tool, for instance, has many physical problems that should be addressed at an early phase of the design process while non modeled phenomena could be compensated at later phase (Fig. 1). Three fundamental components are required to generate any movement in a machine: the guideways, the bearings, and the actuator. The guideways will support the moving parts of the system. The linearity and stiffness are the main key parameters. The bearings play the role of interface between the moving part and the guideways; they require specific stiffness and damping. The generation of motion is secured by a third important component that is the actuator, for which a number of key design parameters are required and discussed later in this paper. The translational or rotational movements have to be kinematically designed.

A number of recent precision actuators designed to generate precision motion in standard machine-tools have been discussed in the literature [1-3] or allowing very small forces, hence low axial stiffness [4, 5]. Extensive work in the design, modeling and control of precision motion with friction compensation has been achieved over recent years [6-10] showing the importance of friction effects and attempts to reduce them. A special interest was focused on applications requiring adaptive and intelligent control schemes for friction compensation techniques [11-16]. A so-called *dual-model strategy* method considered as very popular method for its simplicity and effectiveness has been proposed in [6, 8, 11].

The model of friction is modeled by a linear spring in the microdynamics and is neglected in the macrodynamics. Two controllers are designed for the two dynamic aspects, respectively. Precision positioning is achieved via the two steps of coarse and fine positioning. But it is difficult to combine the two controllers to work together [17]. Adaptive control laws for friction compensation have been proposed by [18] [19] relying heavily on linear parameterization of nonlinear dynamic models of friction. An application

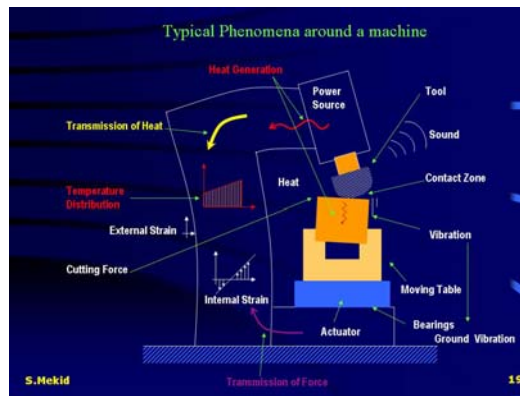
---

<sup>†</sup> This paper was recommended for publication in revised form by Associate Editor Jeonghoon Yoo

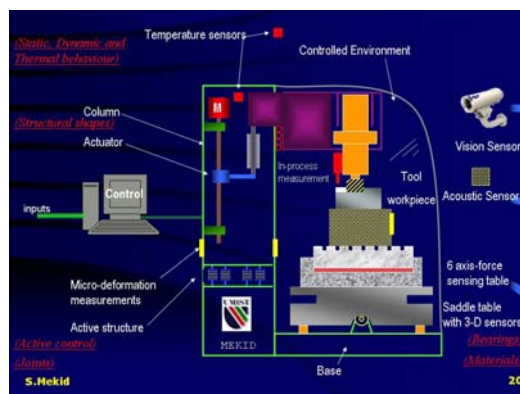
\*Corresponding author. Tel.: +966 3 860 7746, Fax.: +966 3 860 7746

E-mail address: smekid@kfupm.edu.sa

© KSME & Springer 2009



(a)



(b)

Fig. 1. (a) Major physical phenomena in a machine tool. (b) Ideal compensated machine.

of the min–max adaptive algorithm for model-based friction compensation [20] in a positioning system using a nonlinear parameterization of the friction model has been reported showing improved friction compensation. The drawback of this adaptive scheme is that the nonlinearly parameterized system must satisfy certain matching criteria. The proportional-integral-derivative (PID) control is usually used. Due to its popularity, there are many papers about the tuning rules and implementation details of the control [21, 22]. However, while more attention is focused on advanced control strategies for friction compensation, application of the PID control for precision positioning has received less attention.

Parallel kinematic machines are introducing various types of joints where friction is required to be compensated for precision positioning. This becomes a challenging task as the frictional model is complex and is distributed over several joints. A few works

have attempted to address this case [23] but an important investigation is to come.

The current paper proposes two aspects in the design of a high precision actuation. A design procedure for an actuator generating high precision motion is presented with a discussion of some important aspects encountered in the design process including mainly contact interface shapes with encountered nonlinearities. The second novel aspect is the way to compensate for induced errors in the controller. These errors could be induced by many sources at first or second order and not necessarily having known models. The internal model control technique proposed in this paper is capable of compensating for the friction and other phenomena that degrade positioning without requiring a governing physical model.

## 2. Actuators and drive selection

A precision actuator is dedicated to generate an accurate and a linear movement. The mechanical component, e.g. the drive mechanism, of the actuator is a very important sub-component as it has to comply with a number of criteria cited below. An electric component is required to deliver sufficient torque and to secure a recommended resolution via an encoder. As the required movement has to be very accurate, these actuators will be designed or chosen according to the following criteria: high stiffness in the active axis, high linearity, no backlash, low disturbances, reverse motion, and high sensitivity to active control. The choice of the drive mechanism is critical to motion system performance. There are many solutions but the most prevalent ones for high performance motion control are given below:

- (a) Lead screw/ball screw with rotary servo motor and encoder.
- (b) Linear servo motor.
- (c) Piezo ceramic linear actuator for short strokes.

The friction drive actuator has been chosen for its high axis stiffness, low lost motion and very good stability. Its implementation in various projects has shown a very good performance. Friction drive systems are generally preferred to several feed drive systems such as ball screw, linear motor, and planetary roller screw. An experimental comparison between the above cited feed drive systems [1] showed that the friction drive is the ideal drive system. It provides motions with low disturbances, no backlash, high stiffness (axial stiffness (e.g. 100 N/ $\mu\text{m}$ )), low

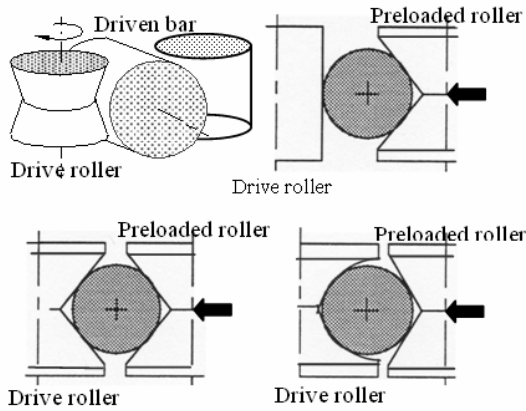


Fig. 2. Rollers configurations.

sliding friction, and low linearity errors. Other design considerations are minimum cost, maximum reliability, minimum heat generation and compact configuration. Nanometer resolution is easily reached [2].

### 3. Friction drives design concepts

Depending on the specifications related to the slide table to be controlled, high stiffness and zero slippage are required together with high mechanical resolution. The material at the interface is very important in this case.

The friction drive’s general configuration (Fig. 2) is composed of a round bar that is kept centered between twin-V rollers, the V geometry, allowing contact points and a double tangential stiffness estimated using Mindlin formulation [29].

Fig. 2 suggests three possible combinations of the interface between the drive shaft and the driven roller for improved tangential stiffness and slippage avoidance. The interface stiffness computation is discussed in section 4-1.

One of the easiest ways to increase the resolution is to consider a small angle between the drive shaft and the driven roller (Fig. 3(b)). The resolution of the friction drive could be estimated in Fig. 3(a) as  $L=\pi D$  while in Fig. 3(b) as  $L=\pi D \cdot \tan(\theta)$ . From the latter principle, Muzimoto [3] has suggested a twist roller that can achieve Angstrom resolution. Fig. 4 shows the twist roller friction drive comprising three rollers to increase the stiffness. The three rollers are slightly inclined (10 to 15 deg.) with respect to the driving shaft which is linked to a motor. The flange is assembled to the moving carriage.

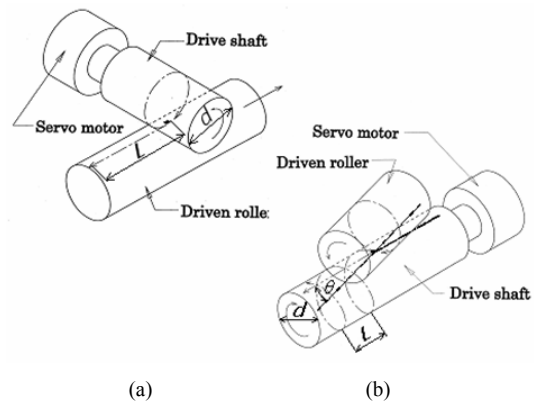


Fig. 3. (a) Conventional friction drive. (b) Angular friction drive.

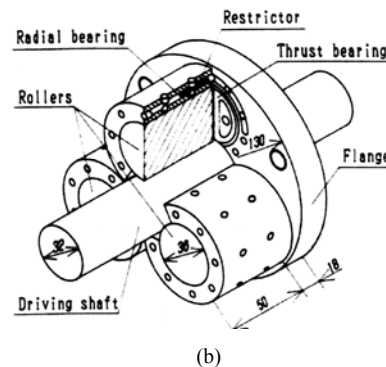
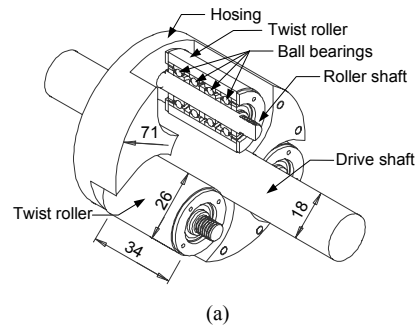


Fig. 4. Twist friction drive with either roller bearings (a) or air bearings (b).

## 4. Design procedure

### 4.1 Stiffness

For any fine positioning with an axial stiffness  $K_T$ , any disturbance force  $F_s$  will introduce an error  $\delta_k$  in the direction of the motion and is estimated as follows:

$$\delta_x = \frac{F_\delta}{K_T} \tag{1}$$

Hence, a larger stiffness induces a lower error. The actuation stiffness is mainly related to the tangential stiffness at the contact interface (Fig. 6). Mindlin [29] has suggested an equation to estimate the stiffness depending on the interface shape.

$$K_T = \frac{4Ea}{(2-\eta)(1+\eta)\Phi} \left(1 - \frac{P_x}{\mu_g P_z}\right)^{\frac{1}{3}} \tag{2}$$

where  $E$  is the Young Modulus,  $a$  is the dimension of the contact point,  $\eta$  is Poisson's coefficient,  $\mu_g$  is the friction coefficient,  $\Phi$  is a function of the contact geometry,  $P_x$  and  $P_z$  are tangential and normal contact pressure.

The preload applied to both rollers preloaded

against the moving shaft is the main parameter to be adjusted to obtain the required contact stiffness and to prevent slippage. This preload could be measured by using a compressive force sensor. The stiffness computation is considered only for interfaces shown in Fig. 2. The stiffness for three different interfaces has been computed for different tangential forces and the results are shown on Table 1. The tangential stiffness is very high (e.g., 120 N/μm) for a hybrid combination, i.e., a curved and a linear interface in V form with four contact points (Fig. 2(d)). It is not certain that this configuration although with high stiffness will deliver a high resolution as the contact interface area is larger than in the case of two V rollers. A high resolution is usually obtained at low speed as stick-slip phenomenon may appear often at high speed depending on the applied preload. The driven bar could be provided with high hardness (60-70 HRC), straightness (4-15 μm/m) and smooth finish (0.25 to

Table 1. Tangential stiffness for various contact interfaces.

| Type   | Tangential Stiffness behavior | Friction drive concepts |
|--------|-------------------------------|-------------------------|
| V-C    |                               |                         |
| V-V    |                               |                         |
| Hybrid |                               |                         |

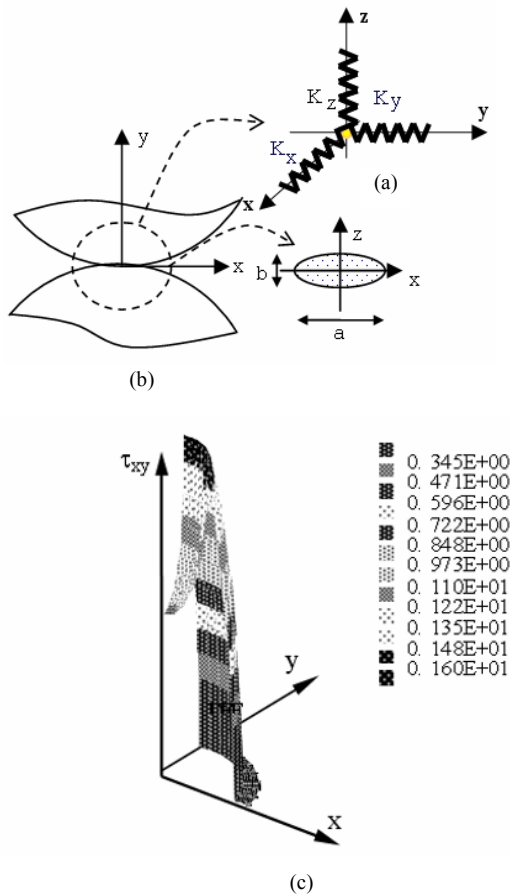


Fig. 5. Interface contact characteristic and distribution of the tangential shear stress at the start of slippage.

0.5 μm Ra). These characteristics should be carefully chosen according to the expected performance. In the case of an angular friction drive (Fig. 3(b)), the tangential stiffness will increase by approximately 1.5% with an angle between 10 to 15 deg.

The birth of the slippage starts from the inner surface of the contact zone (Fig. 5(c)). If the contact zone is circular, then the slippage evolves in a concentric surface with respect to the contact zone as simulated in Fig. 5(c). These references [24, 25] are interesting for indepth information.

The shear stress at a distance ρ from the center is estimated [29] as:

$$\tau_x(\rho) = \begin{cases} \frac{3}{2} \mu_g \frac{P_z}{\pi a^2} \left( 1 - \frac{\rho^2}{a^2} \right)^{1/2}, & \text{if } a_0 < \rho < a; \\ \frac{3}{2} \mu_g \frac{P_z}{\pi a^2} \left( 1 - \frac{\rho^2}{a^2} \right)^{1/2} - \frac{3}{2} \mu_g \frac{P_z}{\pi a^2} \left( 1 - \frac{\rho^2}{a_0^2} \right)^{1/2} \frac{a_0}{a}, & \text{if } \rho < a_0. \end{cases} \quad (3)$$

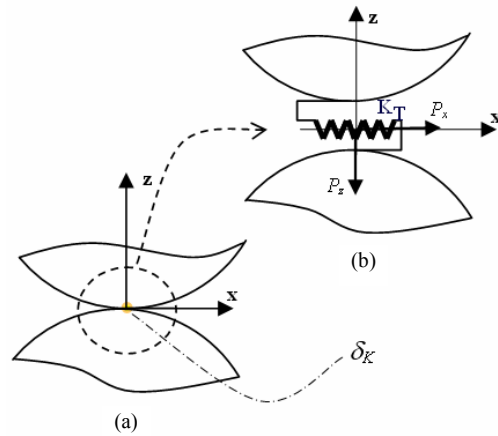


Fig. 6. Tangential stiffness model.

where μ<sub>g</sub> is the friction coefficient; P<sub>z</sub>, the normal force; a, the radius of the contact zone; and a<sub>0</sub>, the initial diameter of slippage area. ρ could be defined as (x<sup>2</sup>+y<sup>2</sup>)<sup>1/2</sup>.

The reaction force could be calculated using expression (4).

$$T_x = \int_0^a \int_0^{2\pi} \tau_x \rho \, d\rho \, d\theta = \mu_g P_z \left( 1 - \frac{a_0^3}{a^3} \right). \quad (4)$$

The dimensioning of the rollers has preferably to meet two criteria:

(i) Hertz contact stress admissible.

$$\frac{P_z}{\pi ab} < P_{HertzMax} \quad (5)$$

where P<sub>z</sub> is the preload; and a, b, are the dimensions of the contact surface.

(ii) Maximum displacement precision avoiding geometric errors on the roller (radius R).

$$R = \Delta \tilde{P} \Delta \Phi \quad (6)$$

where ΔΦ is the encoder resolution and ΔP the required resolution.

From the point of view of control, the minimum stiffness could be estimated as follows. If M is the weight of the moving part in a machine and K the axial actuator stiffness, the time constant of the system is estimated as:

$$\tau_{\text{sys}} = 2\pi \sqrt{\frac{M}{K}} \quad (7)$$

The servo controller loop time should be faster than this time constant. For a controller of  $N$  bits of DAC resolution (generally estimated from the required resolution in displacement), the increment of force the actuator could offer will be:

$$\Delta F = \frac{F_{\text{max}}}{2^N f(\tau_{\text{sys}}, \tau_{\text{servo}})} \quad (8)$$

where  $f$ , is a function relating the time constant and the servo control performance. This depends on the transfer function used in the controller.

Hence, the minimum required stiffness for a deformation (or error)  $\delta_k$  caused by  $K$ , will be:

$$K > \frac{F_{\text{max}}}{2^N \delta_k f(\tau_{\text{sys}}, \tau_{\text{servo}})} \quad (9)$$

#### 4.2 Particular parasitic errors in straightness and linearity

Other possible errors such as form errors may occur from the geometric errors of the manufactured actuator components, but also from errors induced by the design concept itself. Fig. 7 shows a comparison between a standard design Fig. 7(a) and a precise design Fig. 7(b) of a friction actuator. The latter has shown far better precision performance than the standard one. This is due not only on the tight tolerances imposed on the components but mainly on new concepts of assembly free from mechanical constraints as shown for the new rail design (i.e., only magnets to maintain the rails in a V shape). Other errors may result from external constraints such as thermal expansion. This could shift the whole roller assembly with respect to the bar creating a lateral force. The following example shows how a lateral induced force  $F_t$  at the edge of the roller, yields a small yaw angle. It is important to observe that the magnitude of this angle  $\theta$  depends on the type of the precision ball bearing arrangement. The measurements performed with the collaboration of SKF in France show in Table 2 the behavior of this angle for “X” and “O” arrangements. Face-to-face arrangement “X” is more suitable in reducing the angle  $\theta$  when the tangential force  $F_t$  increases.

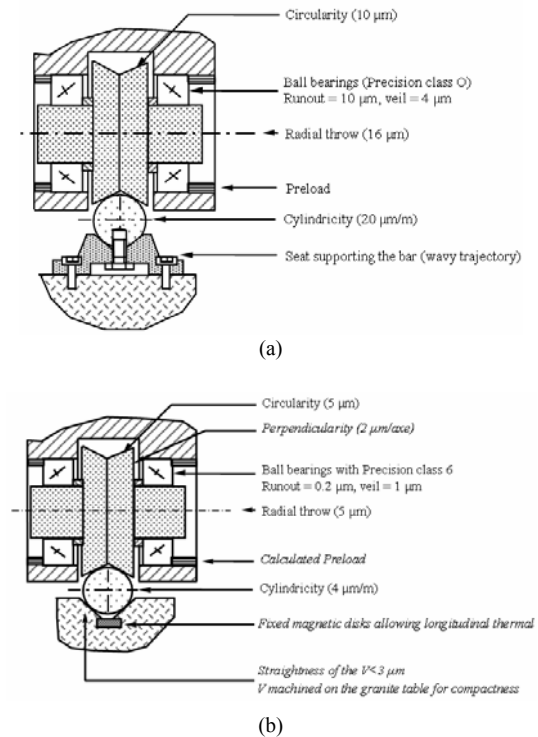


Fig. 7. Standard and Precision Rolling assembly configuration (extra features are in italic in (b)).

#### 4.3 Dynamic analysis

The main purpose of the dynamic analysis is to determine the first natural frequencies and to check their locations with respect to the control bandwidth as well as the mode of vibration.

The latter may act in the direction of the motion and hence affects the quality of the movement. It is important to avoid this parasitic mode. The next concern is to compare the dynamic stiffnesses of the actuation and the actuated object for the same mode of vibration. An example is given in Table 3.

##### 4.3.1 Frequency and modes of vibration

The actuator has been modeled by FEM and its first natural frequencies have been calculated.

The first frequency is near the controller bandwidth (e.g., 45 Hz), but its mode of vibration is a yaw movement with very small effects on the main motion because the carriage will not be affected dynamically as it is seen in Table 3.

##### 4.3.2 Effects on the carriage stiffnesses

The carriage stiffness has been computed based on

Table 2. Variation of the angle with respect to the tangential force.

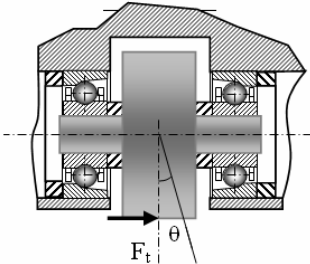
|  | Bearings arrangement                   | $F_t = 5 \text{ N}$                    | $F_t = 10 \text{ N}$                   | $F_t = 50 \text{ N}$                  |
|---|--|--|--|---------------------------------------|
|   | “X”                                    | $\theta = 11.6 \text{ } \mu\text{rad}$ | $\theta = 8.7 \text{ } \mu\text{rad}$  | $\theta = 2.9 \text{ } \mu\text{rad}$ |
| “O”   | $\theta = 14.5 \text{ } \mu\text{rad}$ | $\theta = 23.3 \text{ } \mu\text{rad}$ | $\theta = 37.8 \text{ } \mu\text{rad}$ |                                       |

Table 3. Comparison of the dynamic stiffnesses between the actuator and the carriage.

| Vibration modes |                 | Carriage Stiffness [N/ $\mu\text{m}$ ] | Actuator Dynamic Stiffness [N/ $\mu\text{m}$ ] |
|-----------------|-----------------|--|--|
| Mode 1          | Flexion /Y axis | 44.5                                   | 25.3   |
| Mode 2          | Pitch           | 67.3                                   | 46.5   |
| Mode 3          | roll            | n/a                                    | 246.7  |

the bearings stiffnesses and their configuration with respect to the guideways. The actuator dynamic stiffnesses for various modes have been extracted from the dynamic analysis and compared as shown in Table 3. It appears that the carriage stiffnesses in the different modes of the vibration will be affected by the friction drive actuator.

#### 4.4 Control

The contact between two solid materials will always lead to non-linearities observed at the pre-rolling in fine positioning. From the point of view of contact mechanics, a model for pre-rolling has been written [26] to take into account the pre-rolling and the rolling resistance. Other effects may not be possible to model, as most of the time these are not known.

Therefore, to compensate dynamically for unmodeled phenomena, an internal model control (IMC) scheme is used. The following sections will introduce the principle.

##### 4.4.1 Mathematical model

The control of a current-driven brushless electrical motor with permanent magnets on the rotor is governed by linear equations. Eq. (10) describes the relation between the angular acceleration of the rotor and the torque developed by the motor.

$$J \frac{d^2 \theta}{dt^2} = C_{em}(t) - C_t(t) \quad (10)$$

Eq. (11) gives the value of the electromotive torque  $C_{em}(t)$  as a function of the statoric current.

$$C_{em}(t) = K_m i(t) \cdot \sin \varphi(t) \quad (11)$$

To simplify the control of the linear slide, the resistive torque  $C_t(t)$  can be considered as a nearly static external disturbance, whose influence will be compensated for by the integral term of the corrector. In addition, we assume  $C_r(t) = 0$  in Eq. (10). The impact of this approximation will be lowered by the great deal of attention paid to the design of the bench and pertaining to the avoidance of all sources of static friction. With this hypothesis, Eqs. (10) and (11) will be combined leading to Eq. (12) which summarizes the behavior of a current-driven brushless motor.

$$J \frac{d^2 \theta}{dt^2} = K_m i(t) \cdot \sin \varphi(t) \quad (12)$$

The functioning of the motor is optimized from the power consumption point of view by setting the angular difference between the statoric and the rotoric magnetic fields  $\varphi(t)$  to  $\pi/2$ .

The optimization is easily achieved with respect to the position of the rotoric field by feeding each statoric coil individually in order to form a homogeneous magnetic field. In this particular application, a rotary incremental encoder with a 12-bit resolution gives the position of the rotor.

If  $\varphi = \pi/2$ , the sinus term of Eq. (12) disappears. Eq. (13), which describes the behavior of a current driven brushless AC motor (with permanent magnets on the rotor) becomes a second order, linear and mono-variable equation suitable for the setting up of a PID controller.

$$J \frac{d^2 \theta}{dt^2} = K_m i(t) \quad (13)$$

4.4.2 Internal model control (IMC)

The effect of unmodeled mechanical behaviors on the quality of the straight motion could be compensated dynamically.

An internal model control scheme (whose global approach of the notion of precision of the model avoids focusing on any specific phenomena or mechanical behavior effects) was added on top of the PID controller. Basically, it consists of introducing into the control a variable characterizing the difference between the output of the process and modeling. Its value is then converted into an image of the extra torque required to compensate unmodeled loads and is added to the motor's command calculated by the PID controller.

This control scheme is presented in Fig. 8 where block M represents the model of the process and  $M^{-1}$  its reverse.  $M^{-1}$  exists and is stable because the model of behavior of the bench (Eq. (13)) was kept single variable and linear and all zeros were eliminated from it through various approximation as detailed in [30]. This Moreover, the calculus of the modeling error is achieved at the acceleration level of the control in order to avoid the presence of integral terms in the model M. It means that the modeling error is considered as the difference between the slide table's translation acceleration predicted by the model and the one measured.

The real acceleration is obtained by a double-numerical derivation of the information provided by the linear incremental encoder. A low-pass numerical filter was used to reduce the amount of high frequency noise introduced by the derivations and focus the action of the IMC loop on very low frequency disturbances. Indeed, if the modeling error calculated

at the sample time  $n$  contains a large amount of numerical noise, when used to modify the value of the motor's command at the time  $n+1$ , it would act as a powerful noise generator, which goes against the initial purpose of the IMC.

The order of the filter was limited to reduce the dephasing. The very low cut-off frequency of the filter does not affect the natural frequency of the control as the IMC loop acts independently of the PID control which determines the dynamic of the servo system (Fig. 9).

Fig. 10 shows the position diagram used by the friction Actuator with a low pass Butterworth filter [27].

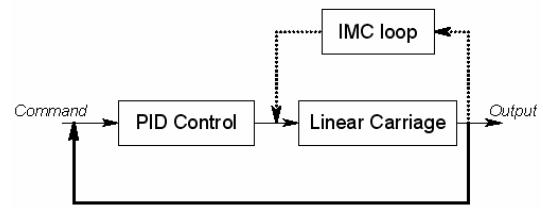


Fig. 8. Principle of the IMC applied to the PID speed control loop.

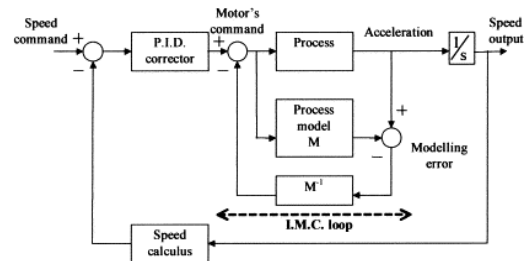


Fig. 9. Representation of separate action of the IMC loop and PID servo control.

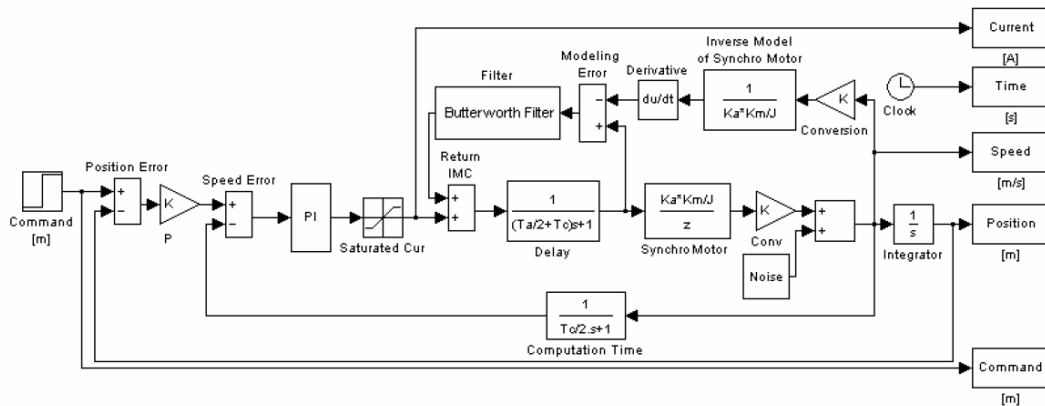


Fig. 10. Position diagram for IMC scheme using Matlab.



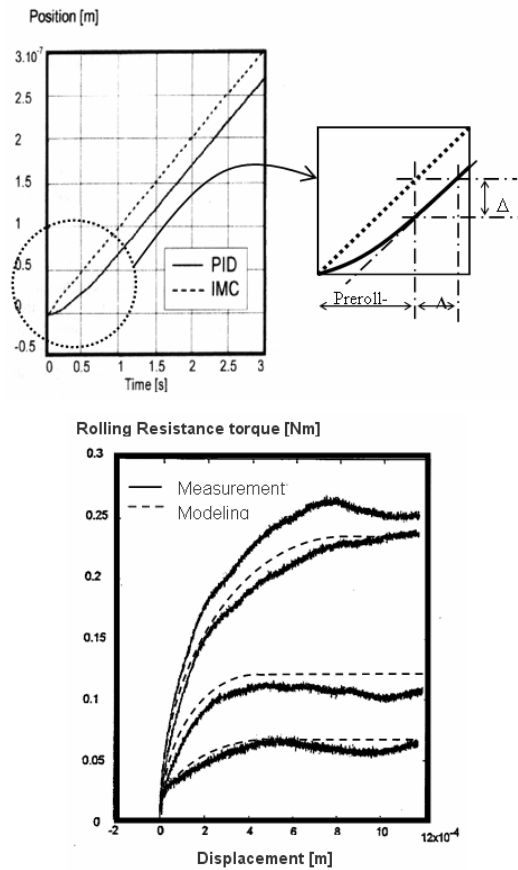


Fig. 11. Error compensation in rolling resistance.

Even at very low speed, rolling resistance induces micro-dynamics, especially when it is submitted to periodical variation of loads (i.e., machining), hence for example, the non-suitability for ultra high precision machining. However, the non-linear behavior takes place at the contact interface and may cause loss of contact at high rolling speed [28]. The rolling resistance could be modeled to predict its evolution as shown in Fig. 11. A model was proposed depending on the type of materials at the interface [26]. The model could be taken into account by the controller. At low speeds, one of the most relevant problems in positioning control is the exhibition of the non-linear behavior at prerolling stage as shown in Fig. 10. The PID controller does not compensate for the phenomena and delays the positioning by  $\Delta t$ . Such an influence is addressed by using an IMC controller instead of PID controller to compensate for temporal delay when it starts rolling. This is also exploited in forward step test avoiding delays (Fig. 14).

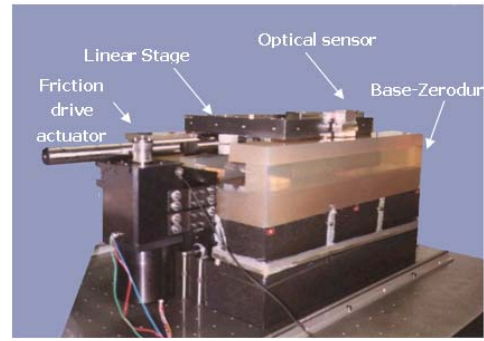


Fig. 12. Configuration of the linear carriage with friction drive.

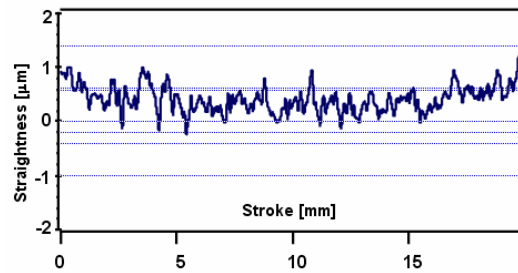


Fig. 13. Straightness measurement on the main axis.

## 5. Experiment and results

The friction drive may be coupled to the base with reinforced flexures to minimize the effects of forced geometric congruence while the traction bar is linked to the carriage at one end via monolithic flexure (Fig. 12). The principle to be respected is that the driving force of the actuator should operate through the axis of reaction. Hence, the slide will not be subject to parasitic forces or Abbé errors unless an offset was considered. The measurement of the straightness over the whole stroke was performed with a laser interferometer.

A variation of less than one micrometer over a stroke of 200 mm was observed with good repeatability (Fig. 13). In terms of positioning resolution, an optical sensor from Heidenhain was used. The following measurement spectrum (Fig. 14 and 15) show a very well resolved motion for continuous and reverse steps of 25 nm and 50 nm.

The displacement shown on the figures is not normalized, hence a noisy response with high frequency chatters are observed mainly for steps of 25 nm.

This is due to the low resolution of the optical probe which noise is evaluated at 16nm. Hence, a

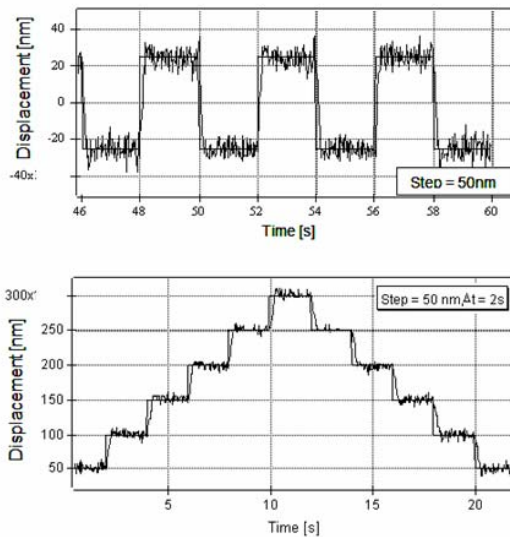


Fig. 14. Reverse and continuous 50 nm step motion response.

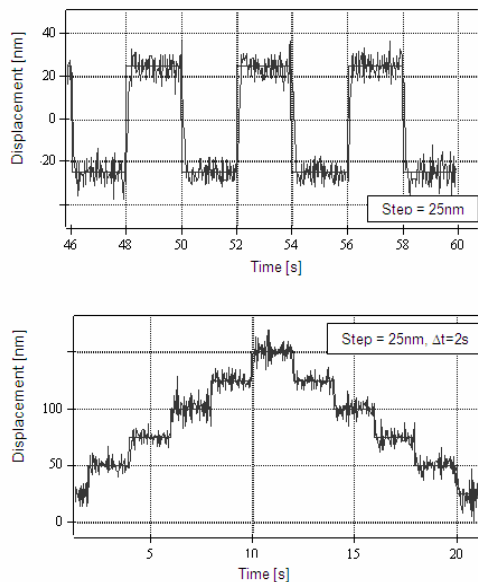


Fig. 15. Reverse and continuous 25 nm step motion response.

band of a minimum of 16 nm amplitude at high frequency (controller positioning) will be seen in all positioning steps.

## 6. Conclusion

Some key aspects in the design of an actuator to generate precision motion were discussed in this paper. A particular focus was made on the friction drive

capabilities. A careful design with attention to details mentioned within this paper will lead to a precise system. The key aspects discussed in this paper are summarized as follows.

- Contact interface and preload.
- Axis stiffness.
- Bearing arrangement to hold the rollers.
- Control strategy to address uncompensated errors.
- Dynamic of the actuator with respect to the carriage.

The static and dynamic stiffnesses correlated from the modes of vibration have to be compared to secure a carriage motion with less parasitic actuator effects. Non-linearities appearing from pre-rolling of the actuator could be eliminated with a dedicated control strategy (e.g., IMC).

A very well resolved motion is achievable at low speed, while it is difficult to do so at high speed. An alternative method would allow slowing down the actuator when approaching targets using a specific regime for speeds and/or acceleration and hence be able to position objects at low speed with high precision and repeatability.

## Acknowledgment

The author wishes to acknowledge KFUPM for its support in providing the various facilities utilized in the preparation of this paper.

## References

- [1] M. Weck and T. Bispink, Examination of high precision slow-motion feed drive systems for sub-micrometer range. Fraunhofer (IPT), internal report, Aachen, (1991).
- [2] S. Mekid and M. Bonis, Conceptual Design and study of high precision translational stages: Application to an optical delay line, *J. American Society for Precision Engineering*, 21 (1) (1997) 29-35.
- [3] H. Mizumoto, M. Yabuya, T. Shimizu and Y. Kami, An angstrom-positioning system using a twist-roller friction drive, *J. American Society for Precision Engineering*, 17 (1) (1995) 57-62.
- [4] S. B. Choi, S. S. Han, Y. M. Han and B. S. Thompson, A magnification device for precision mechanisms featuring piezoactuators and flexure hinges: Design and experimental validation, *Mechanism and Machine Theory*, 42 (9) (2007) 1184-1198.

- [5] J. D. Kim and S. R. Nam, An improvement of positioning accuracy by use of piezoelectric voltage in piezoelectric driven micropositioning system simulation, *Mechanism and Machine Theory*, 30 (6) (1995) 819-827.
- [6] H. Tachikawa, M. Fukuda, K. Sato and A. Shimokohbe, Ultra precision positioning using air bearing lead screw. *Trans JSME Ser C*, 66 (2000) 1559-1566.
- [7] B. Armstrong-Helouvry, P. Bupont and C. C. De Wit, A survey of models, analysis tools, and compensation methods for the control of machines with friction. *Automatica*, 7 (1994) 1083-1093.
- [8] S. Futami, A. Furutani and S. Yoshida, Nanometer positioning and its micro-dynamics. *Nanotechnology*, 1, (1990) 31-37.
- [9] C. C. De Wit, H. Olsson, K. J. Astrom and P. Lischinsky, A new model for control of systems with friction, *IEEE Trans Automatic Control*, 3 (1995) 419-425.
- [10] P. I. Ro, W. Shim and S. Jeong, Robust friction compensation for submicrometer positioning and tracking for a ball-screw-driven slide system. *J. American Society for Precision Engineering*, 2 (2000) 160-173.
- [11] P. I. Ro and P. I. Hubbe, Model reference adaptive control of dual-mode micro/ macro dynamics of ball screws for nanometer motion. *J Dyn Syst Meas Contr*, 115 (1993) 103-108.
- [12] C. L. Chao, J. Neou, Model reference adaptive control of air-lubricated capstan drive for precision positioning. *J. American Society for Precision Engineering*, 4 (2000) 285-290.
- [13] J. H. Ryu, J. Song and D. S. Kwon, A nonlinear friction compensation method using adaptive control and its practical application to an in-parallel actuated 6-DOF manipulator. *Contr Eng Pract* 2 (2001) 159-167.
- [14] L. R. Ray, A. Ramasubramanian and J. Townsend, Adaptive friction compensation using extended Kalman–Bucy filter friction estimation. *Contr Eng Pract* 2 (2001) 169-179.
- [15] Y. H. Kim and F. L. Lewis, Reinforcement adaptive learning neural-net-based friction compensation control for high speed and precision. *IEEE Trans Contr Syst Technol*, 1 (2000) 118-126.
- [16] J. T. Teeter, M. W. Chow and J. J. Brickley, Novel fuzzy friction compensation approach to improve the performance of a DC motor control system. *IEEE Trans Ind Electron*, 1 (1996) 113-120.
- [17] J. Mao, H. Tachikawa and A. Shimokohbe, Precision positioning of a DC-motor-driven aerostatic slide system, *J. American Society for Precision Engineering*, 27 (1) (2003) 32-41.
- [18] J. J. Craig, P. Hsu and S. S. Sastry, Adaptive control of mechanical manipulators. *The International Journal of Robotics Research*, 6 (2) (1987) 16-28.
- [19] Canudas de Wit and Astrom (1987).
- [20] A. M. Annaswamy, F. P. Skantze and A. P. Loh, Adaptive control of continuous time systems with convex/concave parametrization. *Automatica*, 34 (1) (1998) 33-49.
- [21] K. J. Astrom and T. Haggglund, The future of PID control. *Contr Eng Pract*, 9 (2001) 1163-1175.
- [22] K. J. Astrom and T. Haggglund, *PID Controllers: theory, design, and tuning*. Research Triangle Park, NC: Instrument Society of America; (1995).
- [23] K. Harib and K. Srinivasan, Kinematic and dynamic analysis of stewart platform-based machine tool structures. *Robotica*, 21 (5) (2003) 541-554.
- [24] K. L. Johnson, *Contact Mechanics*, University of Cambridge, 1989.
- [25] J. J. Kalker, *Three Dimensional Elastic Bodies in Rolling Contact*, Kluwer Academic Publishers, (1990).
- [26] S. Mekid, A Non-linear Model for Pre-Rolling Friction Contact in Ultra Precision Positioning, *Journal of Eng. Tribology, Proc of IMechE*, 218 Part J (2004) 305-311.
- [27] O. Olejniczak, PhD thesis, Compiègne University, France, (1994).
- [28] S. Mekid and M. Bonis, Numerical Resolution of the Contact Vibration under Harmonic Loads, In *Contact Mechanics - Computational Techniques*, Southampton, UK: Computational Mechanics Publications, (1993) 61-67.
- [29] R. D. Mindlin, Compliance of elastic bodies in contact, *J. of Applied Mech. Trans ASME*, 71 (1949) 259-268.
- [30] Y. Okazaki, T. Bispink, M. Weck, Proceedings of the 3rd International Conference on Ultraprecision in Manufacturing Engineering, Aachen, Germany, (1994).



**Samir Mekid** received his MSc and PhD in Precision Engineering in 1988 and 1994, respectively, from Compiègne University of Technology (France). He is a member and Chartered Engineer (CEng) from IMechE. Samir Mekid was

a faculty member at UMIST then the University of Manchester (UK) and currently at KFUPM (KSA). He is engaged in multidisciplinary research including precision machine design, instrumentation, sensors and metrology. His research is supported by various National and European funded projects. His recent edited book entitled *Introduction to Precision Machine Design and Error Assessment* by CRC press has recently been published.